Egypt. J. Chem. **Vol. 67,** No. 1 pp. 225 - 238 (2024)

Egyptian Journal of Chemistry

http://ejchem.journals.ekb.eg/

Preparation, Characterization, and Spectroscopic Properties of a Novel Iron (III), Copper (II), and Nickel (II) Complexes with Schiff base ligand derived from salicylaldehyde and p–phenylene diamine on Polyvinyl chloride photodegradation

E. A. Mohamed [1,2#], N. A. Negm [2#], A.O. Youssef [3], G. H. Sayed [3*]

[1-]Global laboratory and Health Care Solutions, Cairo, Egypt, [2]- Egyptian Petroleum Research Institute, Nasr City, Cairo, Egypt. [3]- Department of Chemistry, Faculty of Science, Ain Shams University, Cairo, Egypt

Abstract

The stabilization of polyvinyl chloride polymer has a great concern for researchers due to its high instability in the environmental conditions of heat and ultraviolet arrays. Herein, three metal complexes of Schiff base ligand were prepared and their chemical structures were confirmed using elemental analysis, FTIR, 1H-NMR, and UV/Vis spectra. The prepared metal complexes were incorporated in PVC as photo-stabilizers. Only 0.5% by weight of these prepared Schiff bases metal complexes was blended with the PVC polymer to form films with a width of (50 µm). The prepared samples were exposed to ultraviolet irradiation time was varied ranging from 0 to 300 h and the impact of irradiation scheduled upon the PVC stabilization was examined each 50 h. The degree of degradation of PVC in the presence and absence of the different stabilizers was determined using various techniques, including the degree of oxygenated compounds formed, degree of unsaturation, viscosity, and degree of deterioration. The results showed that in the native PVC, the degradation progressively increased over time at the conditions of the experiments. The addition of the stabilizers decreased the degradation considerably. The formation of carbonyl, hydroxyl, and unsaturated intermediates was decreased in the presence of Cu-L, and Ni-L. While Fe-L stabilizer showed weak efficiency. The reasons for the stabilization and the mechanism of the degradation/stabilization processes were discussed based on the electronegativity of the metal ions and the antioxidant activities of the different metal complexes.

Keywords: Schiff base; Metal complex; polyvinyl chloride; Photostabilizer; antioxidant.

1. Introduction

Polyethylene, polypropylene, and polyvinyl chloride (PVC) are produced and used in huge quantities [1]. PVC is one of the most important and used polymers due to its outstanding physical and chemical properties, low production cost, and diverse applications of packaging to devices [2,3]. Rigid PVC is utilized in water pipes, windows, doors, floor tiles, and credit cards [4]. Flexible PVC is used as a replacement for rubber in curtains, raincoats, and packaging films [5]. weak thermal stability of PVC [6,7] leads to polymer damage and deterioration [8]. Irradiation of PVC by ultraviolet irradiation at 250-350 nm wavelength for a long time of exposure leads to observable changes in color and mechanical properties accompanied by a sharp reduction in its molecular weight and tensile strength, which shortens its using life [9,10]. Oxygenated containing intermediates, polyenes, and chlorophyll residues are produced under ultraviolet irradiation and lead to the photodegradation process [11,12]. So, it is important to photo-stabilize PVC polymer to increase its lifetime during use as a final product [13]. Several photo-stabilizers containing aromatic derivatives were used in the protection of PVC against the photodegradation process [14,15]. Photostabilization is a process used to protect PVC from degradation by preventing and/or slowing the photodegradation reaction of the polymer by degrading threats [16]. Photostabilization of PVC is performed through two kinds of stabilizers [17]: the first is the primary stabilizers which can inhibit the allylic chlorides production during the photodegradation process of PVC, and the second is the secondary stabilizers

Corresponding authors: ethoo.azmy@gmail.com

Receive Date: 11 May 2023, Revise Date: 04 July 2023, Accept Date: 12 July 2023

DOI: 10.21608/EJCHEM.2023.210265.7963

which can scavenge the chloride radicals and hydrogen chloride produced during the degradation process [16,18]. Consequently, the production of a new substance that performs as an effective additive for enhancement of PVC photostability because of their capability for hydrogen chloride, and chloride radicals scavengers produced during the photodegradation process of PVC chains [19]. Nonetheless, in the two past decades, Numerous PVC additives have been synthesized and studied as photo stabilizers counting inorganic chemical salts [20,21], hetero-cycles compounds [11,22], aromatics [23-25], and titanium dioxide [25,26]. These compounds display extraordinary effectiveness toward inhibition of the photodegradation process of PVC afterward long period exposure of to ultraviolet light. However, these compounds have insufficient characteristics during application for their stabilizing role, as these are unstable, fast-degradable, and harmful to health and the environment [27]. Metal complexes were more efficient and lake from the disadvantageous of the above-reported stabilizers for PVC [28,29]. Schiff base compounds are vital compounds and suitable ligands during the formation of metal complexes with a wide range of transition metal ions to produce versatile types of stable metal complexes those suitable for different applications [31,32]. Herein, we presented the technique for synthesis and characterization of three metal complexes of iron (III), copper (II), and nickel (II) with Schiff base ligand derived from salicylaldehyde and p-phenylene diamine and their function as photo stabilizers for PVC polymer. The prepared Schiff bases have highly aromatic characters, easy to prepare, stable, non-volatile, and cost-effective..

2. EXPERIMENTAL

2.1 Materials and techniques

All chemicals were analytical grade and were purchased from Sigma-Aldrich, and were used as received without further purification.

Melting points were measured on Gallen Kamp, the elemental analysis was conducted using Vario-Elementar, FTIR spectra were recorded using Fourier transform infrared spectroscopy (FTIR) Thermo Electron Nicolet 7600 (USA) IR-spectrophotometer, ^{1}H-NMR spectra at 300 MHz on GEMINI-300-BB NMR spectrometer using tetramethyl silane as an internal standard in deuterated dimethyl sulfoxide (DMSO-*d*6), Electronic spectral changes in electron distribution between ligand-metal in complexes were recorded in the wavelength range of 200-700 using a Jasco V-670 UV/Vis spectrophotometer. Film thickness was measured using micrometer type 2625 A, Germany. Weathering tests were performed using Xenotest 440 utilizes XenoLogic™.

2.2 Synthesis

2.2.1 Synthesis of Schiff bases

p-phenylene diamine (0.01 mole) and salicylaldehyde (0.02 mole) were mixed in 250 mL one necked flask in the presence of absolute ethyl alcohol (20 ml) as a solvent and a few drops of glacial acetic acid as a dehydrating agent. The reaction medium was refluxed at reflux temperature for 120 minutes, and then the reaction medium was settled to precipitate the product at room temperature for 24 hours. The solid product was filtered and recrystallized from ethanol to afford the proposed Schiff base (N, N′-Bis(Salicylidene)-p-phenylene diamine, L) **(*Scheme 1*).**

L ($C_{20}H_{16}N_2O_2$): Yield 88%; orange crystals recrystallized from chloroform; mp. 208-210 ^{o}C; UV/Vis (DMSO, nm): 280, 390; FTIR (KBr) (υ, cm^{-1}): 3467 (O-H), 1608 (C=N); ^{1} H-NMR (DMSO-*d*6) δ:13.20 (s, 2H), 8.66 (m, 2H), 7.42 (m, 4H), 7.28 (s, 4H), 7.02 (m, 4H). Anal. Calc.: C, 75.9%; H, 5.1%; N, 8.8%; Found (%): C, 75.4%; H, 5.06%; N, 8.7%.

2.2.2 Synthesis of metal complexes

The metal complexes of the prepared ligand were prepared according to the following procedures: ethanolic solutions of the different metal ions precursors (ferric chloride, copper acetate, and nickel chloride) were prepared by dissolving 0.01 mole of the metal salts in 100 mL absolute ethanol and mixed individually with ethanolic solution contains 0.02 mole of L under stirring at reflux temperature for 360 minutes and left for precipitation at room temperature overnight. The formed colored metal complexes were filtered off, washed several times with ethanol, and left to dry at 40 ^{o}C for 24 hours under a vacuum.

$Fe(L)_3Cl_3$: Yield (85%); Black ppt, Anal. Calc. For $C_{60}H_{48}N_6O_6Cl_3Fe$ (%): C, 64.9%; H, 4.35%; Fe, 5.03%; N, 7.56%; Found (%): C, 64.4%; H, 4.3%; Fe, 4.98%; N, 7.5%; FTIR (KBr) (υ, cm^{-1}): 1660 (C=O), 1605 (C=N), 530 (Fe-O), 450 (Fe-N), UV/Vis (DMSO, nm): 285 (π-π*), 360 (n-π*).

$Cu(L)_2(OAc)_2$: Yield (86%); Brown ppt, Anal. Calc. For $C_{44}H_{38}CuN_4O_8$ (%): C, 64.9%; H, 4.7%; Cu, 7.8%; N, 6.88%; Found (%): C, 64.4%; H, 4.67%; Cu, 7.71%; N, 6.79%; FTIR (KBr) (υ, cm^{-1}): 1640 (C=O), 1607(C=N), 1456, 1225 (OAc),751 (Cu-O), 548 (Cu-N), UV/Vis (DMSO, nm): 290 (π-π*), 340 (n-π*).

Ni(II)$(L)_2(ClO_4)_2$: Yield (88%); Yellow ppt, Anal. Calc. For $C_{40}H_{32}Cl_2Ni\ N_4O_{12}$ (%): C, 53.9%; H, 3.62%; Ni, 6.59%; N, 6.29%; Found (%): C, 53.5%; H, 3.6%; Ni, 6.55%; N, 6.25%; FTIR (KBr) (υ, cm^{-1}): 1608 (C=N), 510 (Ni-N), 455 (Ni-O), UV/Vis (DMSO, nm): 280 (π-π*), 380 (n-π*).

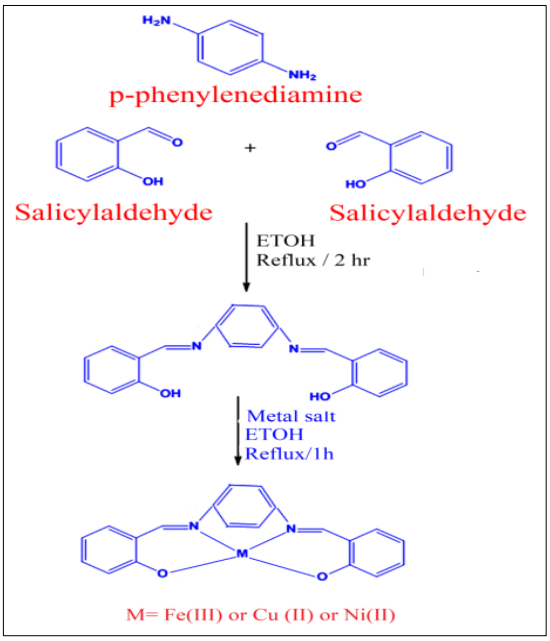

Scheme 1: Synthetic route of Schiff base ligand (L) and corresponding Iron (III), Copper (II), and Nickel (II) complexes.

2.2.3 Preparation of polymer films

PVC film preparation was preceded according to the following steps. First, 5 g of PVC was dissolved in 100 mL of tetrahydrofuran until complete homogeneity of the produced matrix. Then, the prepared metal complexes were added to the polymer/THF matrix (0.5% by weight of PVC) and stirred at 500 rpm for 30 minutes for complete homogeneity. Polymer films with different additives were prepared by placing the polymer solution in uniform petri-dishes on a balanced surface to maintain the uniformity of the film thickness and allowed to slow dryness in the closed chamber at room temperature [31]. The obtained film thickness was 0.25 mm for all samples.

2.3 Accelerated weathering of PVC films

Degradation of PVC films was performed under accelerated weathering conditions. The accelerated weathering was performed at 75% humidity under UV irradiation from a UV lamp that emitted UV radiation wavelength in the range of 290 nm to 360 nm. Samples were placed horizontally to the incident light for 180 minutes (equivalent to 1-week natural weathering conditions), and then films were collected and stored in a dry and dark place for further measurements [32].

2.4 Determination of the rate of photodegradation

The photodegradation of the bank and stabilized PVC films was monitored using FTIR spectroscopic analysis during the range of 4000-400 cm^{-1}. The degree of degradation was followed throughout monitoring three main absorption bands: the unsaturation (C=C) at 1600 cm^{-1}, carbonyl groups (C=O) at 1720 cm^{-1}, and hydroxyl groups (-OH) at 3450 cm^{-1}. The extent of photodegradation was determined from the variation in the index of the three absorption bands determined from their intensities, and the data were compared relative to the intensity of the absorption band corresponding to CH_2 at 1310 cm^{-1} as a reference band. Three indexes were calculated using the corresponding transmittance of FTIR spectra of the formed groups namely: $I_{C=C}$, $I_{C=O}$, and I_{OH} according to Beer–Lambent law (I_s: group index, A_s the area under the peak of group band, and A_r: area of reference group) [33], ***Equation 1.***

$$Is = \frac{As}{Ar} \qquad (1)$$

2.5 Determination of the average molecular weight

The variations in the molecular weight of stabilized and unstabilized PVC polymer samples after photodegradation were followed by measuring the variation in the viscosity of their solution using an Ostwald glass viscometer. In this method, the exact weights of the polymer samples were dissolved in 100 mL of THF and the viscosity [γ] at room temperature was used to calculate the average weights of the different polymers using the Mark-Houwink equation [34] (***Equation 2***).

$$[\gamma] = KM^{\alpha}{}_{v} \qquad (2)$$

K, α: constants related to solvent and polymer at a definite temperature.

2.6 Determination of the antioxidant activity of metal complexes

2.6.1 DPPH Assay

The antioxidant performance of Fe-L, Cu-L, and Ni-L metal complexes was proceeded using two methods using 2,2-diphenyl-1-picrylhydrazyl (DPPH) radical scavenging and hydrogen peroxide assays. In 2,2-diphenyl-1-picrylhydrazyl (DPPH) radical scavenging, Fe-L, Cu-L, and Ni-L metal complexes in methanol at a concentration of 9×10^{-3} M were mixed individually in 3 mL of DPPH solution in methanol at a concentration of 1×10^{-4} M.

The metal complexes-DPPH mixtures were incubated at room temperature in dark for 30 minutes. The antioxidant activities of the metal complexes were determined by measuring the intensities of absorption of the different targeted mixtures at 517 nm; using UV/Vis spectrophotometer (Beckman Coulter), to detect the remaining amounts of DPPH radicals in the solutions. The antioxidant activity (AA %) was calculated according to ***Equation 3*** [35].

$$\text{Inhibition, AA\%} = [[A_{DPPH^\bullet} - A_{sample}]/A_{DPPH^\bullet}] \times 100 \quad (3)$$

where A_{sample}: absorbance at 517 nm for DPPH$^\bullet$ solution after the addition of metal complexes, $A_{DPPH^\bullet}$: absorbance at 517 nm for DPPH$^\bullet$ solution. All experiments were performed in triplicate.

2.6.2 ABTS$^+$ radical scavenging assay

2,2-azinobis(3-ethylbenzothiazoline-6-sulfonic acid) (ABTS$^+$) radical-scavenging assay of the synthesized Fe-L, Cu-L, and Ni-L metal complexes was evaluated following the procedures of Giao et al., [36]. ABTS$^+$ assay comprises the formation of ABTS$^+$ chromophore through the oxidation reaction of ABTS$^+$ using $K_2S_2O_3$. The scavenging assay of Fe-L, Cu-L, and Ni-L metal complexes on the formed ABTS$^+$ radical cation was measured using spectrophotometric measurements at a wavelength of 734 nm. The reaction began as a result of adding diluted ABTS$^+$ (1 mL) to various doses (5–100 µg/mL) of Fe-L, Cu-L, and Ni-L metal complexes (10 µL) and the control sample was ethanol (10 µL). The antioxidant activity (AA %) was calculated according to ***Equation 4***.

$$AA\% = [[A_o - A_1]/A_o] \times 100 \quad (4)$$

A_o, A_1: absorbance intensities of control and sample solutions at 734 nm, respectively.

3. Results and discussion

3.1 Characterization

3.1.1 Electronic spectral and magnetic susceptibility studies

The electronic absorption spectra of the prepared ligand (L) and related metal ion complexes of Fe(III), Cu(II), and Ni(II) were recorded at 10^{-3} M concentration in DMF solution at room temperature over the wavelength range of 200-800 nm (***Figure 1***) [37]. The ligand (L) exhibits two intense absorption bands. The first absorption band was located at a shorter wavelength of 270-272 nm, which was ascribed to the π-π* transition of azomethine and benzene ring [38]. The second absorption band allocated 329-331 nm, which is assigned for n-π* transition of the lone pair electrons of the C=N bond [39]. The behaviors of the prepared metal complexes were provided with two main characteristics. Firstly, the shifting of the parent bands to higher wavelengths; secondly, the appearance of a new absorption band corresponded to *the d–d* transition appeared in the visible domain at a longer wavelength [40].

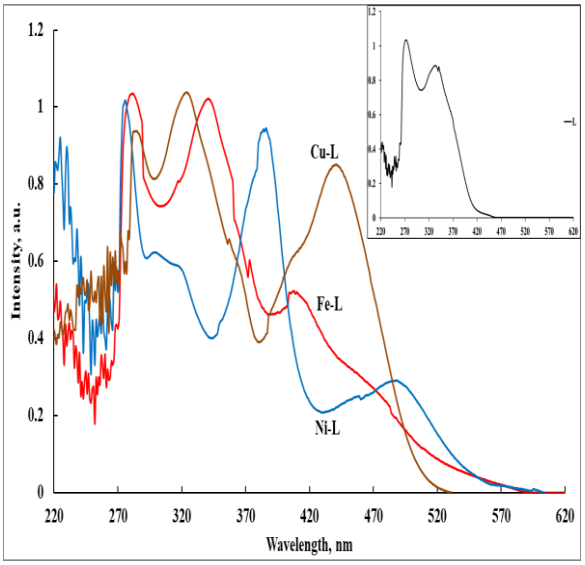

Figure 1: UV-Vis. Spectra of the prepared ligand (L), and the corresponding metal complexes (M-L).

The three metal complexes showed their characteristic absorption bands (*Figure 1*), where the Fe-L metal complex (d^5 configuration) showed bands at 279, 338, and 405 nm; the Cu-L complex showed three absorption bands at 283 nm, 320 nm, and 438 nm, while Ni-L showed its bands at 275, 384 and 485 nm. The intra-ligand transition bands were characterized for the prepared metal complexes; in the case of the Fe-L complex, the bands appeared at 279, and 338 nm; at 283 nm and 320 nm for the Cu-L metal complex; and at 275 and 384 nm for Ni-L complex. The band at 405 nm, allocated to the spin and parity forbidden $^6A_{1g} \rightarrow T_{2g}$ transition of Fe(III) ion in an octahedral conformation [41]. The high-spinning octahedral Fe(III) complex shows an extremely low band intensity corresponding to the *d-d* transition. The detected magnetic moment of the Fe-L complex at 5.62 B.M. suggests a high spins conformation of the Fe ion with its unpaired electrons (5e). The band of Cu-L at 438 nm was ascribed as a result of *d-d* spin allowed transition for $^2A_{1g} \rightarrow {}^2B_{g2}$ and $^1A_{g2} \rightarrow {}^1B_{g2}$ [42]. The magnetic moment of the Cu-L complex found at 1.14 B.M corresponded to the

single unpaired electron in the outer *d*-orbital, which confirms its square planar conformational arrangement. In the case of the diamagnetic Ni-L complex, the band at 485 nm was due to charge transfer, as a result of *d-d* transition for $^1A_{1g} \rightarrow {}^1A_{2g}$ and $^1A_{1g} \rightarrow {}^1B_{1g}$ which is indicative of the square planar conformation [43].

3.2 Antioxidant efficiency of metal complexes

The oxygen scavenging activities of Fe-L, Cu-L, and Ni-L metal complexes compared to DPPH free radical was evaluated [44]. After 30-min contact of DPPH• solution with the three metal complexes, the absorbance of DPPH• significantly declined compared to pure DPPH• (**Figure 2**).

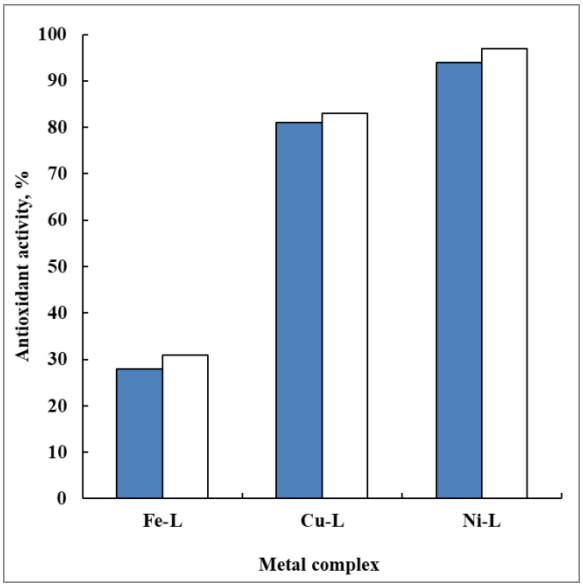

Figure 2: Antioxidant activity of Fe-L, Cu-L, and Ni-L metal complexes using (blue) DPPH radical, and (while) ABTS+ radical scavenging assays.

It is clear that the Fe-L metal complex showed the highest absorption intensity at 517 nm, which was accompanied by the lowest antioxidant activity at 28%. Cu-L and Ni-L metal complexes resulted in lower absorption intensities at 517 nm with corresponding antioxidant activities of 81% and 94%, respectively.

The results were confirmed using ABTS+ radical scavenging assay [45], which showed comparable results to the DPPH assay, **Figure 2**. From the obtained antioxidant activities of the two assays, the antioxidant activities of the synthesized metal complexes can be sorted in the following manner: Ni-L > Cu-L > Fe-L.

3.3 FTIR spectral data of ligand, metal complexes, and compounded PVC

FTIR of ligand showed main peaks at 3340 cm^{-1} due to (N-H) [46,47], 1630 related to azomethine group (C=N) [48,49], and 1581 cm^{-1} owing to aromatic stretches. Comparison of the FTIR chart of ligands and their Fe, Cu, and Ni complexes usually provides an impression about the coordination sites of ligands in the complexes. The stretching vibration band of N-H was detected at 3340 cm^{-1} [50,51]. While in the metal complex's spectra displayed a weak as well as broad peak in the same site that can be attributed to existing of water molecules in the crystal lattice or hydrated water. While the band of the azomethine group (C=N) was found to be shifted to shorter wavenumbers (blue shift) in comparison with the chart of the metal complexes [52]. The blue shift of azomethine of the ligand (1630 cm^{-1}) in the metal complexes (1520–1600 cm^{-1}) designates that the complexion reaction takes place via a coordination bond between the lone pair of electrons on the nitrogen atom of azomethine [53].

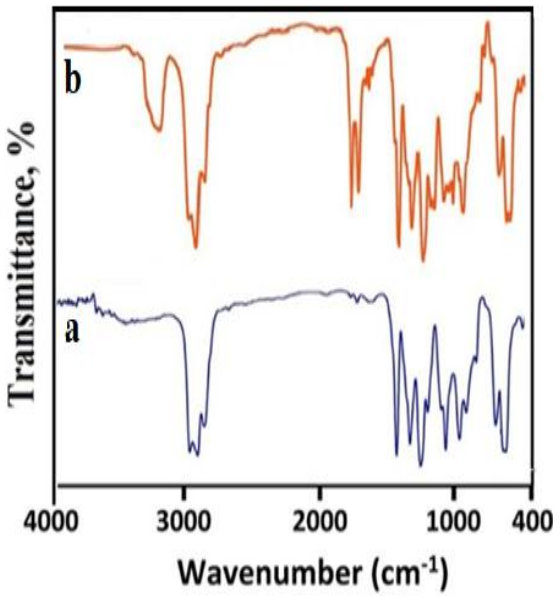

Figure 3: FTIR spectra of pure PVC before (a), and after (b) photodegradation with irradiated time 50 h at 313 nm.

Figure 3 represented the FTIR spectrum of pure un-degraded PVC, which showed several characteristic absorption bands. The peaks at 2920 cm^{-1} and 2970 cm^{-1} represent asymmetric and symmetric stretching vibrations of the C-H bond of the methylene groups (CH2) [21,54]. The absorption peaks around 1410 cm^{-1} were assigned for the bending of the aliphatic C-H bond [55]. The peak at 1260 cm-1 was accredited for the bending of the C-H bond close to Cl. The characteristic absorption bands in the range of 1050-

1150 cm^{-1} are designated for the C-C stretching bond of the PVC chain. The various absorption bands located at the range of 620-660 cm^{-1} correspond to the stretching of C-Cl bonds [56].

Upon performing the photodegradation process for pure PVC polymer, several new absorption bands appeared. Inspecting the spectral data of degraded PVC showed the appearance of three characteristics. The first bands at 1608 cm^{-1} identified the formation of unsaturated bonds of -C=C- resulting from the dehydrohalogenation (-HCl) of the polymer chains [51]. The second appeared around 1735 cm^{-1} representing the combination of free oxygen with the polymer chains in the form of carbonyl compounds (-C=O) [57,58]. While the third characteristic absorption band appeared at 3440 cm^{-1} representing the formation of oxygenated derivatives in the form of hydroxyl groups (-OH) [59,60]. The creation of these three absorption bands proved the occurrence of the degradation process of PVC segments which leads to the elimination of hydrogen chloride molecules and oxidation of the intermediate into carbonyl and hydroxyl products.

Figure 4 represented the FTIR behaviors of the three PVC samples stabilized with 0.5% of Fe-L, Cu-L, and Ni-L metal complexes after performing the photodegradation process at an irradiation wavelength of 313 nm for 50 hours. It is clear that the three characteristic bands at 1608 cm^{-1}, 1735 cm^{-1}, and 3450 cm^{-1} appeared in different intensities. The intensities of these absorption bands were considerably dependent on the type of metal ions. Considering the 1608 cm^{-1} absorption band, the highest intensity was observed in the case of the Fe-L metal complex, while a slight decrease was obtained in its intensity in the presence of Cu-L. On the other hand, a considerable depression in intensity occurred upon using the Ni-L metal complex. The same trends of band intensities variation were observed for 1735 cm^{-1} and 3450 cm^{-1}.

The intensities of the three characteristic absorption bands corresponding to the degradation process of PVC polymer were studied at different process times, and their values were used to determine the extent of degradation during the photodegradation process.

During the photodegradation of PVC films, unsaturated compounds are produced. Thus, the unsaturation index ($I_{C=C}$) can be linked to the irradiation time in the presence and absence of these additives.

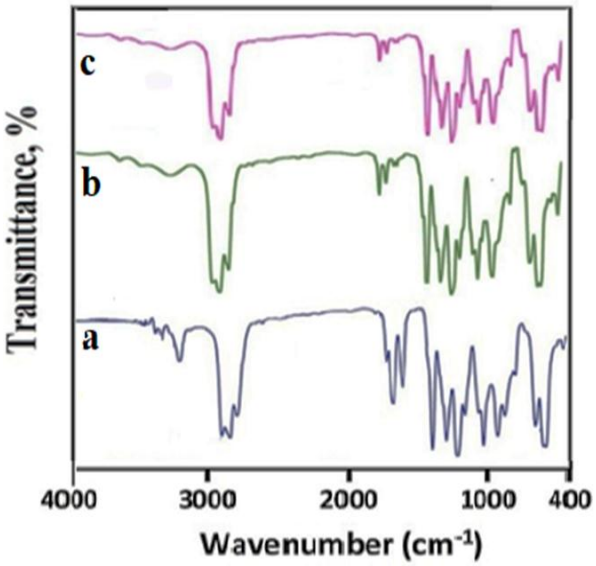

Figure 4: FTIR spectra of PVC blended films after 50 h at 313 nm, Where (a) PVC-Fe-L (b) PVC-Cu-L, and (c) PVC-Ni-L

Furthermore, hydroxyl derivatives are created during the photo-degradation of PVC. Accordingly, the hydroxyl index (I_{OH}) was monitored with irradiation time for PVC and with additives [61].

Figures 5A-C represented the variation in the unsaturation, carbonyl, and hydroxyl indexes of PVC degradation by increasing the time of photo-irradiation. The absorption intensities were used to calculate the carbonyl index (ICO), unsaturation index (Ic=c), and hydroxyl index (IOH), and it is reasonable to accept the fact that the upsurges of these indexes are a measure of the degradation extent. Obviously, the addition of the prepared metal complexes in the PVC matrix led to a noticeable reduction in the degradation of PVC upon irradiation. It is clear that there are two factors influencing the process of degradation, or the tendency of metal complexes stabilization performed on the polymer segments during the process.

The first is increasing the time of the process, which increased the degradation extent of the polymer as represented by increasing the Ic=c, Ic=o, and I-oH. The second is the type of metal ions in the metal complexes. The Ic=o of PVC-Fe-L, PVC-Cu-L, and PVC-Ni-L values were lower than the obtained value of pure PVC film.

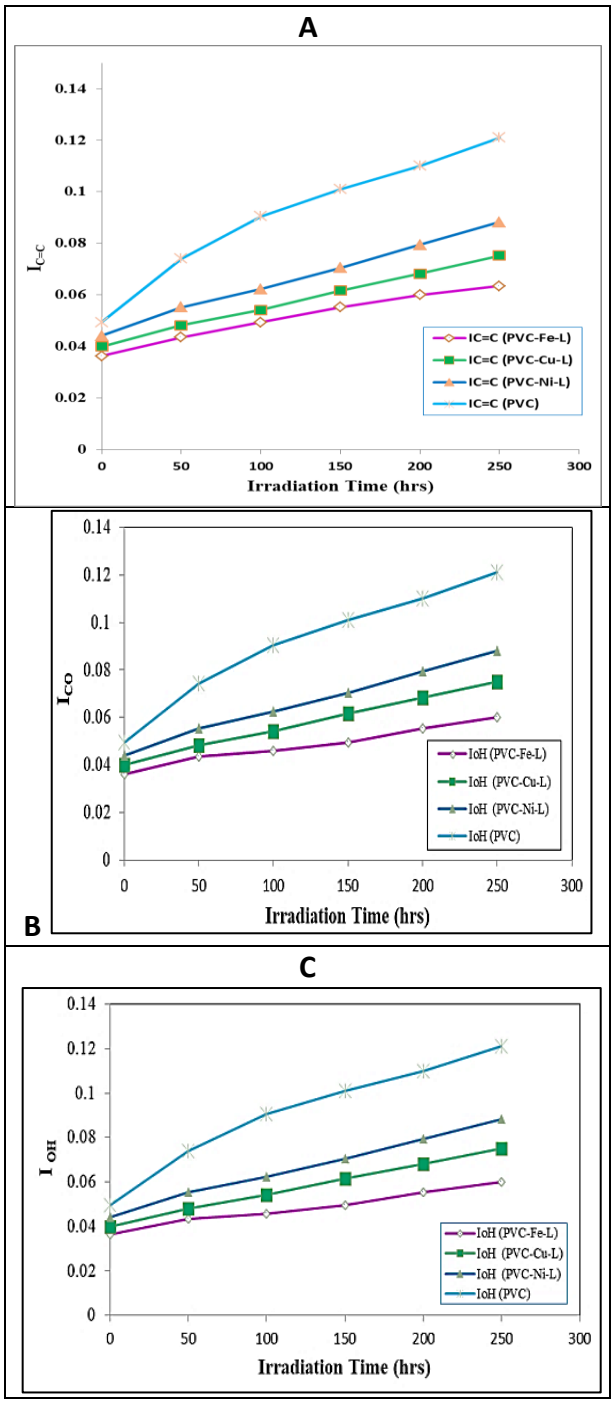

Figure 5: Variation of: (A) the unsaturation index, (B) carbonyl index, and (C) hydroxyl index of PVC degradation as a function of irradiation time.

It is suitable to conclude that the prepared metal complexes could be considered efficient photo stabilizers of PVC polymer. The efficient photostabilizer has a more extended induction period. Consequently, PVC-Ni-L is the most effective photo stabilizer, followed by PVC-Cu-L and PVC-Fe-L which are the least active.

3.4 Molecular weight study of compounded PVC

The degradation of PVC polymer segments is generally accompanied by chain scission followed by photo-oxidation [62], which is responsible for the decrease in the average molecular weight (M_v) of the used polymer.

The viscosities of irradiated solutions in THF of pure and stabilized PVC polymer were measured by viscometer, and their M_v values were calculated using ***Equation 5*** [63].

$$[\eta] = 1{:}63x10^{-2}\, M^{0.766} \qquad (5)$$

The solution of the high molecular weight polymer (un-degraded polymer) has a high viscosity value compared with the degraded polymers. The viscosity of the different compounded PVC formulations was followed in order to determine the change in the average molecular weights in the presence of the synthesized stabilizers and compared them with the unstabilized PVC polymer.

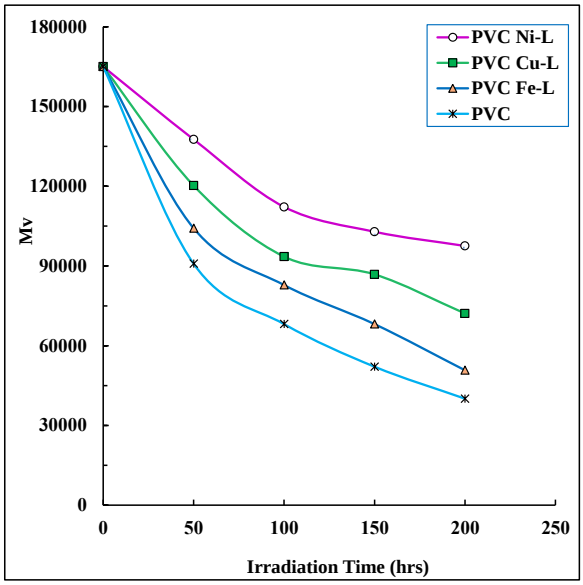

Figure 6: Variation of the average molecular weight M_v during irradiation of unstabilized and stabilized PVC films with 0.5 wt% of stabilizers.

Figure 6 represents two main features of the pure and compounded PVC polymer. First, the gradual increase in the irradiation time from 0 to 250 hours decreased the average molecular weight of the polymer. Second, at constant irradiation time, the unstabilized PVC polymer has the highest decrease in the average molecular, while the type of stabilizers used played a considerable role in their M_v.

MV for blank PVC was at 165,000 before photodegradation (t = 0), but this value was reduced to 99000 after 50 h and reached its minimum value

after 200 h at 40800. MV values of PVC stabilized by Fe-L, Cu-L, and Ni-L after 50 h of irradiation were 104000, 120000, and 137000, respectively. Elevated depressions in the average molecular weights were determined after 200 hrs at 50700, 72100, and 97500 in the case of Fe-L, Cu-L, and Ni-L, respectively. After the irradiation process, the M.V. for the blank PVC film reduced to about 24%, compared to 31%, 44%, and 60% when PVC polymer stabilized by Fe-L, Cu-L, and Ni-L metal complexes, respectively. Based on Mv measurements, Ni-L performs the highest stability for PVC rather than Cu-L, and finally, the least stabilizing efficiency was obtained by using Fe-L as a photostabilizer.

For better support of this view, the number of average chain scission (average number cut per single chain) (S) was calculated using ***Equation 6*** [64]:

$$S=(Mv(t=0) / Mv(t)) - 1 \qquad (6)$$

Mv(t=0), Mv(t): average molecular weight at t=0, t, respectively.

While the degrees of deterioration of the polymer segments as a result of the photodegradation process due to the influence of UV irradiation were determined and represented in ***Figure 7*** using ***Equation 7***.

$$\alpha = (m.S) / M_v \qquad (7)$$

where *m* is the initial molecular weight.

Analyzing the data in ***Figures 7, and 8*** revealed that the pure PVC polymer has a high instability towards the photo-irradiation and a considerable deterioration occurred on its segments, which resulted in a high chain scission that leads to cross-linking in the final product. Furthermore, the calculated degree of deterioration is increased by the time of irradiation. On contrarily, the addition of the synthesized metal complexes to act as photo-stabilizers considerably decreased the polymer chain scission and decreased the degree of deterioration to a large extent [65]. Deep sight in the data revealed that the metal complexes have the following upsurge order of stabilization for PVC polymer as follows: Ni-L > Cu-L > Fe-L.

3.5 Suggested mechanisms of photo stabilization of PVC

The degradation of PVC occurred due to several factors including thermal of photochemical factors. These factors initiate the first step of PVC degradation, which is the formation of the free radical on the polymer segment. The formation of free radicals is the main reason for polymer degradation either during thermal or photochemical treatment.

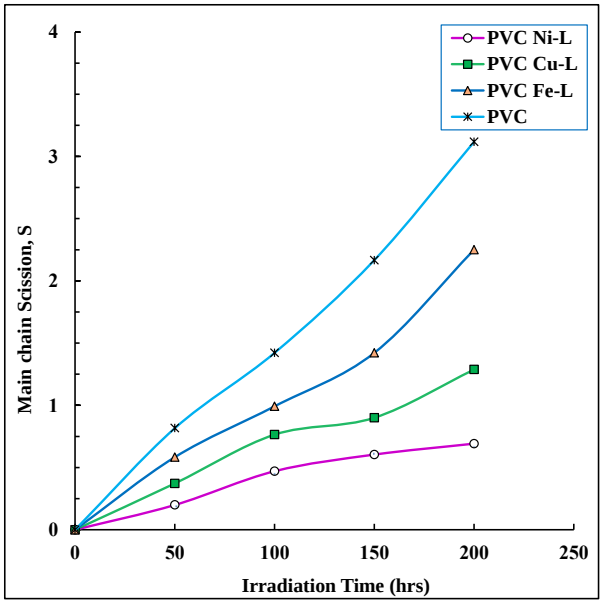

Figure 7: Variation of the main chain scission (S) during irradiation of unstabilized and stabilized PVC films with 0.5 wt% of stabilizers.

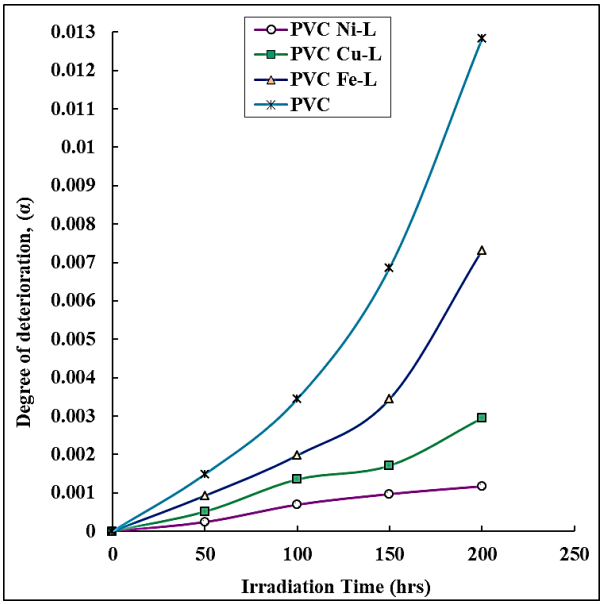

Figure 8: Variation of the degree of deterioration (α) during irradiation of unstabilized and stabilized PVC films with 0.5 wt% of stabilizers

The formed free radicals (***Scheme 2***) follow several reaction routes depending on the environment and the contaminants in the surroundings. The first is the dehydrochlorination reaction which is initiated by the influence of the formed acid (HCl) leading to the

elimination of several protons and chloride ions from the neighboring carbon atoms in a so-called zipper reaction [66].

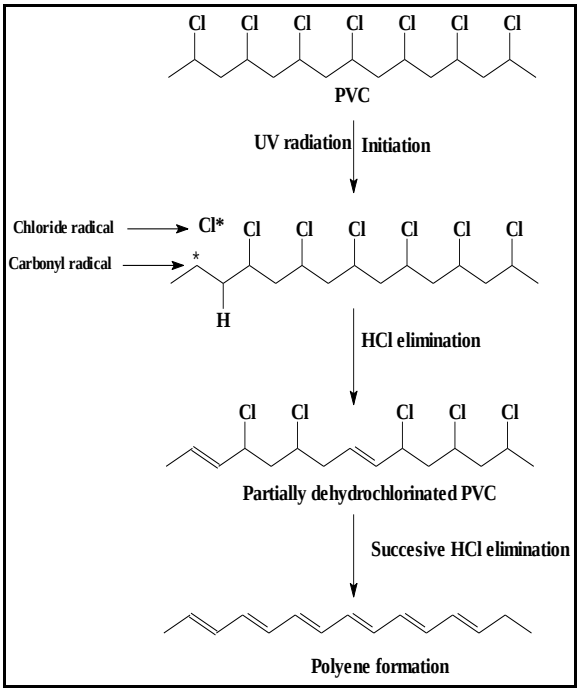

Scheme 2: Photodegradation of PVC into polyene degradation products.

This process resulted in the formation of polyene derivatives. The formation of polyene products leads to the darkness of the polymer color and can be detected using FTIR spectroscopy (***Scheme 2***). Increasing the intensity of FTIR spectra of PVC polymer indicates a high degradation extent of the polymer [67]. The extent of degradation determined by polyene factor $I_{C=C}$ is increased by increasing the degrading factor as can be seen in ***Figure 5A*** for virgin polymer. The second route is the capture of atmospheric oxygen by free radicals to form peroxide derivatives (***Scheme 3***). The chemical instability of the formed peroxides leads to their fragmentation to produce several oxygenated degradation products including aldehydes, ketones, and alcohols. The degree of degradation of PVC based on the second route can be determined spectrophotometrically using FTIR spectra by inspecting the functional groups of C=O, and C-OH and determining the corresponding $I_{C=O}$, and I_{OH} (***Figure 4***). The above two routes lead to one result which is the chain scission of the polymer segments. That harms the mechanical properties of the polymer in terms of depressing the viscosity of the polymer. Decreasing the viscosity of the polymer indicate that the molecular weight of the polymer is decreased. High depression in viscosity indicates the high deterioration of the polymer [68]. The roles of the polymer stabilizers either thermal or photo-stabilizers are to eliminate the formed hydrogen chloride to deactivate the dehydrochlorination process; and to capture the formed free radicals to prevent the formation of peroxide intermediates [69].

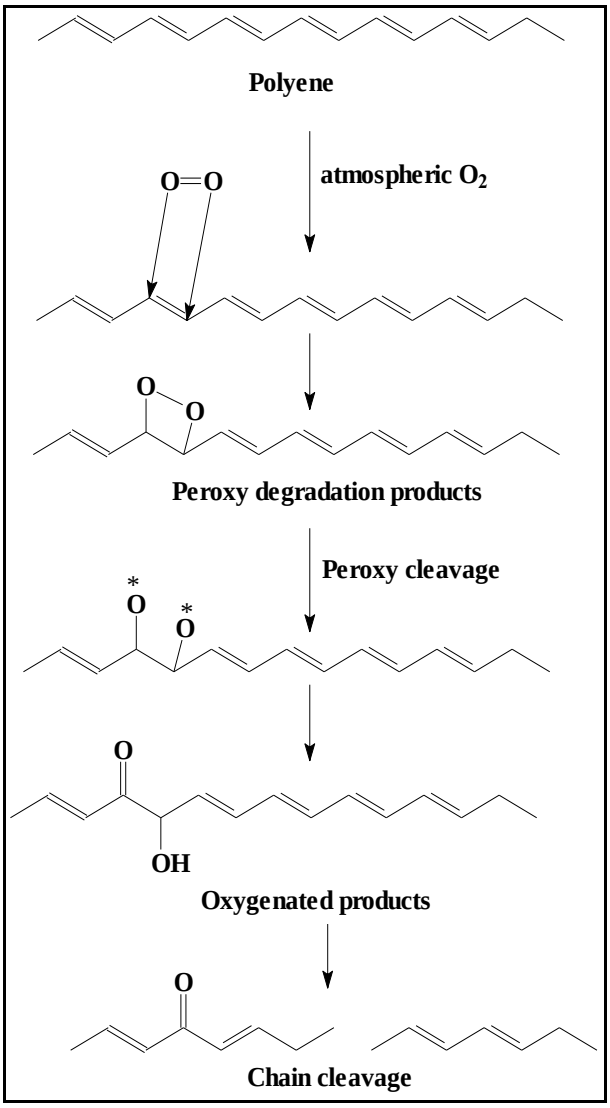

Scheme 3: Photodegradation of PVC into oxygenated degradation products

The prepared metal complexes were used as photo stabilizers during the photodegradation of the PVC polymer. The mechanism of inhibiting these stabilizers can be pointed out in two points. The first is the elimination of the formed hydrogen chloride during the degradation of the polymer by combination with transition metal ions incorporated in the different metal complexes (**Scheme 4**). The second is the capture of the formed free radicals via their incorporation in the electronic cloud of the Schiff bases. The prepared Schiff bases comprise three structural phenyl rings in conjugated form,

which enhance the capture of the formed free radicals. Additionally, the antioxidant activities of the prepared stabilizers showed their high tendencies towards prevention of the oxidation of the degradation products, mainly the polyene products. The comparison between the efficiencies of the photostabilizing activities of the prepared metal complexes arranged them in the following trend: Ni-L > Cu-L > Fe-L. That was ascribed based on the electronegativity of the metal ions. Electronegativity refers to the ability of an atom to attract shared electrons in a covalent bond [70]. The higher the value of the electronegativity, the more strongly that element attracts the electrons. The electro-negativities of the metal ions were as follows: Ni (1.91 eV), Cu (1.9 eV), and Fe (1.83 eV) [71]. As represented from these values, Ni metal ion has the highest ability towards capturing the electrons of the formed free radicals or the oxo-radicals, followed by Cu ions and finally Fe ions.

4. Conclusions

Metal complexes of the prepared Schiff base obtained from the coupling of *p*-phenylene diamine and salicylaldehyde represented diverse behaviors during the stabilization of PVC polymer. Fe-complex exhibited weak stabilization, while Cu- and Ni-complexes showed increased stabilization against the photodegradation of PVC. The stabilizing properties were ascribed to the high antioxidant activity and the ability for capturing the formed carbocations and chloride free radicals during the degradation process. FTIR and viscosity measurements determined the degree of deterioration, intermediates, and functional groups formed on the polymer segments.

5. Conflicts of interest

Authors of manuscripts confirm that there is no conflict of interest of this study with other studied.

6. Formatting of funding sources

There is no funding to declare

7. Acknowledgments

The authors would like to acknowledge the Egyptian Petroleum Research Institute (EPRI) for their

8. References

[1] R.A. Haddad, R. Alsayed, D.S. Ahmed, M. Bufaroosha, N. Salih, S.A. Mohammed, E. Yousif, Environmental performance of coordination complexes as PVC photostabilizers, Mater. Today Proc. 42 (2021) 2849–2852. https://doi.org/https://doi.org/10.1016/j.matpr.2020.12.733.

[2] W. Li, Z. Bai, T. Zhang, Y. Jia, Y. Hou, J. Chen, Z. Guo, L. Kong, J. Bai, W. Li, Comparative study on pyrolysis behaviors and chlorine release of pure PVC polymer and commercial PVC plastics, Fuel. 340 (2023) 127555. https://doi.org/https://doi.org/10.1016/j.fuel.2023.127555.

[3] T. Kameda, Y. Fukuda, G. Grause, T. Yoshioka, Chemical modification of flexible and rigid poly(vinyl chloride) by nucleophilic substitution with thiocyanate using a phase-transfer catalyst, Mater. Chem. Phys. 124 (2010) 163–167. https://doi.org/https://doi.org/10.1016/j.matchemphys.2010.06.011.

[4] Z. Hadj amar, S.F. Chabira, M. Sebaa, Thermal aging effects on the microstructure of rigid PVC tubes used for water transportation in sub-Saharan region, Mater. Today Proc. 49 (2022) 1035–1040. https://doi.org/https://doi.org/10.1016/j.matpr.2021.09.025.

[5] B. Jiang, X. Chang, G. Yan, J. Wang, L. Cui, B. Zhu, X. Tang, F. Meng, Liquid-crystalline behavior and magnetorheological effect of PVC-based ionic polymers with tetrachloroferrate anions, J. Mol. Liq. 359 (2022) 119269. https://doi.org/https://doi.org/10.1016/j.molliq.2022.119269.

[6] J. You, Z. Jiang, H. Jiang, J. Qiu, M. Li, H. Xing, J. Xue, T. Tang, A "Plasticizing-Foaming-Reinforcing" approach for creating thermally insulating PVC/polyurea blend foams with shape memory function, Chem. Eng. J. 450 (2022) 138071. https://doi.org/https://doi.org/10.1016/j.cej.2022.138071.

[7] Y. Zhou, B. Xue, W. Zhang, R. Wang, Prediction of bulk mechanical properties of PVC foam based on microscopic model:Part I-Microstructure characterization and generation algorithm, Polym. Test. 117 (2023) 107872. https://doi.org/https://doi.org/10.1016/j.polymertesting.2022.107872.

[8] H. Asadi, J. Uhlemann, N. Stranghoener, M. Ulbricht, Tensile strength deterioration of PVC coated PET woven fabrics under single and multiplied artificial weathering impacts and cyclic loading, Constr. Build. Mater. 342 (2022) 127843. https://doi.org/https://doi.org/10.1016/j.conbuildmat.2022.127843.

[9] T. Linda, S. Muthupoongodi, X. Sahaya Shajan, S. Balakumar, Photocatalytic Degradation of Congo Red and Crystal Violet Dyes on Cellulose/PVC/ZnO Composites under UV Light Irradiation, Mater. Today Proc. 3 (2016) 2035–2041.

https://doi.org/https://doi.org/10.1016/j.matpr.2016.04.106.

[10] X. Li, X. Duan, S. Chen, H. Chen, A macromolecular PVC plasticizer with enhanced antimigration and excellent UV-shielding performance, Mater. Lett. 327 (2022) 133034. https://doi.org/https://doi.org/10.1016/j.matlet.2022.133034.

[11] T. Saleh, E. Yousif, E. Al- Tikrity, M. Bufaroosha, A. Husain, M.H. Al-Mashhadani, Modification of PVC with captopril and complexation reaction for preparing photostability and thermal stability of PVC, Mater. Sci. Energy Technol. 5 (2022) 311–323. https://doi.org/https://doi.org/10.1016/j.mset.2022.07.001.

[12] Z. Ouyang, Z. Zhang, Y. Jing, L. Bai, M. Zhao, X. Hao, X. Li, X. Guo, The photo-aging of polyvinyl chloride microplastics under different UV irradiations, Gondwana Res. 108 (2022) 72–80. https://doi.org/https://doi.org/10.1016/j.gr.2021.07.010.

[13] M.H. Al-Mashhadani, D.S. Ahmed, H. Adil, A. Ahmed, H. Thamer, B.A. Hamad, M. Abdallh, A. Ahmed, M. Bufaroosha, S.A. Mohammed, N. Salih, R.M. Yusop, E. Yousif, A quantitative spectroscopic study of the bleaching phenomena in photo-stabilized formulations containing PVC exposed to outdoor conditions, Mater. Today Proc. 42 (2021) 2686–2692. https://doi.org/https://doi.org/10.1016/j.matpr.2020.12.705.

[14] S.A. Mahdi, A.A. Ahmed, E. Yousif, M.H. Al-Mashhadani, A. Ahmed, H. Hashim, A.H. Jawad, New organic PVC photo-stabilizers derived from synthesised novel coumarine moieties, Mater. Sci. Energy Technol. 5 (2022) 278–293. https://doi.org/https://doi.org/10.1016/j.mset.2022.04.002.

[15] M. Sabaa, E. Oraby, A. Abdel-Naby, Anthraquinone derivatives as organic stabilizers for rigid poly(vinyl chloride) against photo-degradation, Eur. Polym. J. - EUR POLYM J. 41 (2005) 2530–2543. https://doi.org/10.1016/j.eurpolymj.2005.05.015.

[16] H. Ghani, E. Yousif, M. Kadhom, W. Abdo, M. Yusop, M. Bufaroosha Al Falasi, Improving the Photostabilization of Poly(vinyl chloride) Using 4-(benzylideneamino)benzenesulfonamide Tin Complex, Sci. Lett. 16 (2022). https://doi.org/10.24191/sl.v16i1.16865.

[17] M.A. Farhan, O.A. Nief, W.B. Ali, New photostabilizers for poly (vinyl chloride) derived from heterocyclic compounds, Eurasian Chem. Commun. 4 (2022) 525–543. https://doi.org/10.22034/ecc.2022.332467.1347.

[18] E. Yousif, A. Hasan, Photostabilization of poly(vinyl chloride) – Still on the run, J. Taibah Univ. Sci. 9 (2015) 421–448. https://doi.org/https://doi.org/10.1016/j.jtusci.2014.09.007.

[19] M.W. Sabaa, R.R. Mohamed, E.H. Oraby, Vanillin–Schiff's bases as organic thermal stabilizers and co-stabilizers for rigid poly(vinyl chloride), Eur. Polym. J. 45 (2009) 3072–3080. https://doi.org/https://doi.org/10.1016/j.eurpolymj.2009.08.018.

[20] H. Kaczmarek, J. Kowalonek, D. Ołdak, The influence of UV-irradiation on poly(vinyl chloride) modified by iron and cobalt chlorides, Polym. Degrad. Stab. 79 (2003) 231–240. https://doi.org/https://doi.org/10.1016/S0141-3910(02)00286-0.

[21] Y. Zhang, T. Sun, D. Zhang, Z. Shi, X. Zhang, C. Li, L. Wang, J. Song, Q. Lin, Enhanced photodegradability of PVC plastics film by codoping nano-graphite and TiO2, Polym. Degrad. Stab. 181 (2020) 109332. https://doi.org/https://doi.org/10.1016/j.polymdegradstab.2020.109332.

[22] E. Yousif, D. S. Ahmed, A. Ahmed, A. Hameed, S. Muhamed, R. Yusop, A. Redwan, S. Mohammed, The effect of high UV radiation exposure environment on the novel PVC polymers, Environ. Sci. Pollut. Res. 26 (2019). https://doi.org/10.1007/s11356-019-04323-x.

[23] A.A. Ahmed, D.S. Ahmed, G.A. El-Hiti, M.H. Alotaibi, H. Hashim, E. Yousif, SEM morphological analysis of irradiated polystyrene film doped by a Schiff base containing a 1,2,4-triazole ring system, Appl. Petrochemical Res. 9 (2019) 169–177. https://doi.org/10.1007/s13203-019-00235-6.

[24] H. Hashim, G.A. El-Hiti, M.H. Alotaibi, D.S. Ahmed, E. Yousif, Fabrication of ordered honeycomb porous poly(vinyl chloride) thin film doped with a Schiff base and nickel(II) chloride, Heliyon. 4 (2018) e00743. https://doi.org/https://doi.org/10.1016/j.heliyon.2018.e00743.

[25] R. Farrar, M. Shapiro, I. Javaid, Photostabilized titanium dioxide and a fluorescent brightener as adjuvants for a nucleopolyhedrovirus, BioControl. 48 (2003). https://doi.org/10.1023/A:1025723316426.

[26] N. Shaalan, N. Laftah, G.A. El-Hiti, M.H. Alotaibi, R. Muslih, D.S. Ahmed, E. Yousif, Poly(vinyl Chloride) photostabilization in the presence of schiff bases containing a thiadiazole

moiety, Molecules. 23 (2018). https://doi.org/10.3390/molecules23040913.
[27] E.T.B. Al-Tikrity, A.A. Yaseen, E. Yousif, D.S. Ahmed, M.H. Al-Mashhadani, Impact on Poly(Vinyl chloride) of trimethoprim schiff bases as stabilizers, Polym. Polym. Compos. 30 (2022) 1–11. https://doi.org/10.1177/09673911221094020.
[28] X. Shi, Z. Chen, X. Liu, W. Wei, B.-J. Ni, The photochemical behaviors of microplastics through the lens of reactive oxygen species: Photolysis mechanisms and enhancing photo-transformation of pollutants, Sci. Total Environ. 846 (2022) 157498. https://doi.org/https://doi.org/10.1016/j.scitotenv.2022.157498.
[29] H. Luo, C. Liu, D. He, J. Sun, J. Li, X. Pan, Effects of aging on environmental behavior of plastic additives: Migration, leaching, and ecotoxicity, Sci. Total Environ. 849 (2022) 157951. https://doi.org/https://doi.org/10.1016/j.scitotenv.2022.157951.
[30] N.A. Negm, A.F. El Farargy, I.A. Mohammad, M.F. Zaki, M.M. Khowdiary, Synthesis and inhibitory activity of Schiff base surfactants derived from tannic acid and their cobalt (II), manganese (II) and Iron (III) complexes against bacteria and fungi, J. Surfactants Deterg. 16 (2013) 767–777. https://doi.org/10.1007/s11743-013-1437-5.
[31] T.J. Kemp, R.A. McIntyre, Transition metal-doped titanium(IV) dioxide: Characterisation and influence on photodegradation of poly(vinyl chloride), Polym. Degrad. Stab. 91 (2006) 165–194. https://doi.org/https://doi.org/10.1016/j.polymdegradstab.2005.04.033.
[32] A.G. Hadi, K. Jawad, G.A. El-Hiti, M.H. Alotaibi, A.A. Ahmed, D.S. Ahmed, E. Yousif, Photostabilization of Poly(vinyl chloride) by Organotin(IV) Compounds against Photodegradation., Molecules. 24 (2019). https://doi.org/10.3390/molecules24193557.
[33] S. Gaumet, J.-L. Gardette, Photo-oxidation of poly(vinyl chloride): Part 2—A comparative study of the carbonylated products in photo-chemical and thermal oxidations, Polym. Degrad. Stab. 33 (1991) 17–34. https://doi.org/https://doi.org/10.1016/0141-3910(91)90027-O.
[34] G. Pepperl, Molecular weight distribution of commercial emulsion grade PVC, J. Vinyl Addit. Technol. 8 (2002) 209–213. https://doi.org/10.1002/vnl.10364.
[35] L. Manzocco, M. Anese, M.C. Nicoli, Antioxidant Properties of Tea Extracts as Affected by Processing, LWT - Food Sci. Technol. 31 (1998) 694–698. https://doi.org/https://doi.org/10.1006/fstl.1998.0491.
[36] M.S. Gião, M.L. González-Sanjosé, M.D. Rivero-Pérez, C.I. Pereira, M.E. Pintado, F.X. Malcata, Infusions of Portuguese medicinal plants: Dependence of final antioxidant capacity and phenol content on extraction features., J. Sci. Food Agric. 87 (2007) 2638–2647. https://doi.org/10.1002/jsfa.3023.
[37] S.S. Kumar, V. Sadasivan, S.S. Meena, R.S. Sreepriya, S. Biju, Synthesis, structural characterization and biological studies of Ni(II), Cu(II) and Fe(III) complexes of hydrazone derived from 2-(2-(2,2-dimethyl-4,6-dioxo-1,3-dioxan-5-ylidene)hydrazinyl)benzoic acid, Inorganica Chim. Acta. 536 (2022) 120919. https://doi.org/https://doi.org/10.1016/j.ica.2022.120919.
[38] M.S. Ghurab, O.A. El-Gammal, M.M. El-Gamil, G.M. Abu El-Reash, Preparation, investigation, DFT, pH-metric and cyclic voltammetry of Cr(III), Fe(III), Co(II), Ni(II) and Cu(II) complexes derived from 2-(2-((2Z,3Z)-3-(hydroxyimino) butan-2-ylidene) hydrazineyl)-2-oxo-N-(pyridin-2-yl) acetamide (H3BYPA) and evaluation o, J. Mol. Struct. 1272 (2023) 134156. https://doi.org/https://doi.org/10.1016/j.molstruc.2022.134156.
[39] H.F. El-Shafiy, Synthesis, spectral, photoluminescence, DFT studies and bioassay of new Fe(III), Co(II), Ni(II), Cu(II) and Zn(II) complexes of 1-ethyl-4-hydroxy-3-(nitroacetyl) quinolin-2(1H)-one, J. Mol. Struct. 1166 (2018) 348–361. https://doi.org/https://doi.org/10.1016/j.molstruc.2018.04.023.
[40] N. Ranjitha, G. Krishnamurthy, H.S. Bhojya Naik, M. Pari, L. Afroz, K.R. Sumadevi, M.N. Manjunatha, Structural elucidation, voltammetric detection of dopamine, molecular docking and biological inspection of novel 4-aminoantipyrine derived Schiff bases in Co (II), Ni (II) and Cu (II) complexes, Inorganica Chim. Acta. 543 (2022) 121191. https://doi.org/https://doi.org/10.1016/j.ica.2022.121191.
[41] M.S. Refat, Spectroscopic and thermal degradation behavior of Cr(III), Mn(II), Fe(III), Co(II), Ni(II), Cu(II) and Zn(II) complexes with thiopental sodium anesthesia drug, J. Mol. Struct. 1037 (2013) 170–185.

https://doi.org/https://doi.org/10.1016/j.molstruc.2012.12.055.

[42] N.A. Anan, S.M. Hassan, E.M. Saad, I.S. Butler, S.I. Mostafa, Preparation, characterization and pH-metric measurements of 4-hydroxysalicylidenechitosan Schiff-base complexes of Fe(III), Co(II), Ni(II), Cu(II), Zn(II), Ru(III), Rh(III), Pd(II) and Au(III), Carbohydr. Res. 346 (2011) 775–793. https://doi.org/https://doi.org/10.1016/j.carres.2011.01.014.

[43] N. Keshtkar, A. Zamanpour, S. Esmaielzadeh, Bioactive Ni(II), Cu(II) and Zn(II) complexes with an N3 functionalized Schiff base ligand: Synthesis, structural elucidation, thermodynamic and DFT calculation studies, Inorganica Chim. Acta. 541 (2022) 121083. https://doi.org/https://doi.org/10.1016/j.ica.2022.121083.

[44] M. Pradeep Kumar, D. Ayodhya, Shivaraj, Novel copper (II) binary complexes with N,O-donor isoxazole Schiff base ligands: Synthesis, characterization, DPPH scavenging, antimicrobial, and DNA binding and cleavage studies, Results Chem. 5 (2023) 100845. https://doi.org/https://doi.org/10.1016/j.rechem.2023.100845.

[45] J. Rumpf, R. Burger, M. Schulze, Statistical evaluation of DPPH, ABTS, FRAP, and Folin-Ciocalteu assays to assess the antioxidant capacity of lignins, Int. J. Biol. Macromol. 233 (2023) 123470. https://doi.org/https://doi.org/10.1016/j.ijbiomac.2023.123470.

[46] H.E. Hashem, A.A. Farag, E.A. Mohamed, E.M. Azmy, Experimental and theoretical assessment of benzopyran compounds as inhibitors to steel corrosion in aggressive acid solution, J. Mol. Struct. 1249 (2022) 131641. https://doi.org/https://doi.org/10.1016/j.molstruc.2021.131641.

[47] A.A. Farag, E.A. Mohamed, A. Toghan, The new trends in corrosion control using superhydrophobic surfaces: a review, (2022). https://doi.org/doi:10.1515/corrrev-2022-0020.

[48] N.A. Negm, A.F. El-Farrargy, I.A. Mohammad, Synthesis and Inhibitory Activity of Schiff base Surfactants Derived from Tannic Acid against Bacteria and Fungi, Egypt. J. Chem. 55 (2012) 367–379. https://doi.org/10.21608/EJCHEM.2012.1163.

[49] N.A. Negm, G.H. Sayed, F.Z. Yehia, O.I.H. Dimitry, A.M. Rabie, E.A.M. Azmy, Production of biodiesel production from castor oil using modified montmorillonite clay, Egypt. J. Chem. 59 (2016) 1045–1060. https://doi.org/10.21608/ejchem.2016.1551.

[50] A.A. Farag, H.E. Abdallah, E.A. Badr, E.A. Mohamed, A.I. Ali, A.Y. El-Etre, The inhibition performance of morpholinium derivatives on corrosion behavior of carbon steel in the acidized formation water: Theoretical, experimental and biocidal evaluations, J. Mol. Liq. 341 (2021) 117348. https://doi.org/https://doi.org/10.1016/j.molliq.2021.117348.

[51] E.A. Mohamed, H.E. Hashem, E.M. Azmy, N.A. Negm, A.A. Farag, Synthesis, structural analysis, and inhibition approach of novel eco-friendly chalcone derivatives on API X65 steel corrosion in acidic media assessment with DFT & MD studies, Environ. Technol. Innov. 24 (2021). https://doi.org/10.1016/j.eti.2021.101966.

[52] N.A. Negm, A.A. Altalhi, N.E. Saleh Mohamed, M.T.H.A. Kana, E.A. Mohamed, Growth Inhibition of Sulfate-Reducing Bacteria during Gas and Oil Production Using Novel Schiff Base Diquaternary Biocides: Synthesis, Antimicrobial, and Toxicological Assessment, ACS Omega. 7 (2022) 40098–40108. https://doi.org/10.1021/acsomega.2c04836.

[53] A.A. Farag, A. Gafar Afif, S.A. Salih, A.A. Altalhi, E.A. Mohamed, G.G. Mohamed, Highly Efficient Elimination of Pb(+2) and Al(+3) Metal Ions from Wastewater Using Graphene Oxide/3,5-Diaminobenzoic Acid Composites: Selective Removal of Pb(2+) from Real Industrial Wastewater., ACS Omega. 7 (2022) 38347–38360. https://doi.org/10.1021/acsomega.2c03150.

[54] H.A. Ahmed, A.A. Altalhi, S.A. Elbanna, H.A. El-Saied, A.A. Farag, N.A. Negm, E.A. Mohamed, Effect of Reaction Parameters on Catalytic Pyrolysis of Waste Cooking Oil for Production of Sustainable Biodiesel and Biojet by Functionalized Montmorillonite/Chitosan Nanocomposites, ACS Omega. 7 (2022) 4585–4594. https://doi.org/10.1021/acsomega.1c06518.

[55] A.A. Altalhi, E.A. Mohamed, S.M. Morsy, M.T.H. Abou Kana, N.A. Negm, Catalytic manufacture and characteristic valuation of biodiesel-biojet achieved from Jatropha curcas and waste cooking oils over chemically modified montmorillonite clay, J. Mol. Liq. 340 (2021) 117175. https://doi.org/https://doi.org/10.1016/j.molliq.2021.117175.

[56] M. Kök, M.E. Pekdemir, E. Özen Öner, M. Coşkun, S. Hekim, MWCNT nanocomposite films prepared using different ratios of PVC/PCL: Combined FT-IR/DFT, thermal and shape memory properties, J. Mol. Struct. 1279 (2023) 134989.

https://doi.org/https://doi.org/10.1016/j.molstruc.2023.134989.

[57] A. Altalhi, H. Hashem, N. Negm, E. Mohamed, E. Azmy, Synthesis, characterization, computational study, and screening of novel 1-phenyl-4-(2-phenylacetyl)-thiosemicarbazide derivatives for their antioxidant and antimicrobial activities, J. Mol. Liq. 333 (2021) 115977. https://doi.org/10.1016/j.molliq.2021.115977.

[58] A.A. Altalhi, S.M. Morsy, M.T.H. Abou Kana, N.A. Negm, E.A. Mohamed, Pyrolytic conversion of waste edible oil into biofuel using sulphonated modified alumina, Alexandria Eng. J. 61 (2022) 4847–4861. https://doi.org/https://doi.org/10.1016/j.aej.2021.10.038.

[59] A. Amer, G.H. Sayed, R.M. Ramadan, A.M. Rabie, N.A. Negm, A.A. Farag, E.A. Mohammed, Assessment of 3-amino-1H-1,2,4-triazole modified layered double hydroxide in effective remediation of heavy metal ions from aqueous environment, J. Mol. Liq. 341 (2021) 116935. https://doi.org/https://doi.org/10.1016/j.molliq.2021.116935.

[60] O.M. Abdel Hafez, R.R. Mohamed, M.T.H. Abou Kana, E.A. Mohamed, N.A. Negm, Treatment of industrial wastewater containing copper and lead ions using new carboxymethyl chitosan-activated carbon derivatives, Egypt. J. Chem. (2021). https://doi.org/10.21608/ejchem.2021.82163.4050.

[61] M.N.A. Al-Jibouri, S.A.H. Al-Ameri, W.M. Al-Jibouri, M.A.K. Al-Souz, Spectroscopic study of the effect of a new metal chelate on the stability of PVC, J. Assoc. Arab Univ. Basic Appl. Sci. 14 (2013) 67–74. https://doi.org/https://doi.org/10.1016/j.jaubas.2012.11.003.

[62] J.R. White, A. V Shyichuk, Effect of stabilizer on scission and crosslinking rate changes during photo-oxidation of polypropylene, Polym. Degrad. Stab. 92 (2007) 2095–2101. https://doi.org/https://doi.org/10.1016/j.polymdegradstab.2007.07.013.

[63E. Yousif, J. Salimon, N. Salih, New photostabilizers for PVC based on some diorganotin(IV) complexes, J. Saudi Chem. Soc. 19 (2015) 133–141. https://doi.org/https://doi.org/10.1016/j.jscs.2012.01.003.

[64] A. V. Shyichuk, J.R. White, Analysis of chain-scission and crosslinking rates in the photo-oxidation of polystyrene, J. Appl. Polym. Sci. 77 (2000) 3015–3023. https://doi.org/10.1002/1097-4628(20000923)77:13<3015::AID-APP28>3.0.CO;2-W.

[65] R. Haddad, Ultra violet spectra studies of polystyrene films in presence of some transition metal complexes with 4-amino-5-pyridyl)-4h-1,2,4-triazole-3-thiol, Orient. J. Chem. 31 (2015) 591–596. https://doi.org/10.13005/ojc/310175.

[66] V.P. Kumar, M.K. Gupta, C. Horgan, T.P. O'Sullivan, Synthesis of the quorum sensing molecule Diffusible Signal Factor using the alkyne zipper reaction, Tetrahedron Lett. 59 (2018) 2193–2195. https://doi.org/https://doi.org/10.1016/j.tetlet.2018.04.071.

[67] A.P. Tüzüm Demir, S. Ulutan, Assessment of degradation of plasticized poly(vinyl chloride) films through polyene formation under isothermal conditions, J. Appl. Polym. Sci. 135 (2018) 1–10. https://doi.org/10.1002/app.46092.

[68] J. Yu, L. Sun, C. Ma, Y. Qiao, H. Yao, Thermal degradation of PVC: A review, Waste Manag. 48 (2015). https://doi.org/10.1016/j.wasman.2015.11.041.

[69] C. Jubsilp, A. Asawakosinchai, P. Mora, D. Saramas, S. Rimdusit, Effects of organic based heat stabilizer on properties of polyvinyl chloride for pipe applications: A comparative study with pb and cazn systems, Polymers (Basel). 14 (2022). https://doi.org/10.3390/polym14010133.

[70] J. Hinze, H. Jaffé, Electronegativity. III. Orbital Electronegativities and Electron Affinities of Transition Metals, Can. J. Chem. 41 (2011) 1315–1328. https://doi.org/10.1139/v63-183.

[71] K.A. Moltved, K.P. Kepp, The Chemical Bond between Transition Metals and Oxygen: Electronegativity, d-Orbital Effects, and Oxophilicity as Descriptors of Metal–Oxygen Interactions, J. Phys. Chem. C. 123 (2019) 18432–18444. https://doi.org/10.1021/acs.jpcc.9b04317.